

Controllable synthesis of graphitic carbon nanostructures from ion-exchange resin–iron complex *via* solid-state pyrolysis process[†]

Lei Wang, Chungui Tian, Baoli Wang, Ruihong Wang, Wei Zhou and Honggang Fu*

Received (in Cambridge, UK) 20th June 2008, Accepted 29th July 2008

First published as an Advance Article on the web 12th September 2008

DOI: 10.1039/b810500f

Graphitic carbon nanocapsules, nanosheets and nanoplates were selectively obtained *via* a solid-state pyrolysis route from various ion-exchange resin–iron complexes.

Carbon nanostructures^{1–5} are of great interest in catalysis, electrics, and biomedicine areas, *etc*. While the classical carbon nanotubes and C₆₀ have been dedicated full-fledged research efforts ranging from fabrication to application,^{6,7} analogous work on graphitic carbon materials with special morphologies, such as graphitic nanosheets and highly curved carbon nanocapsules, are comparatively limited. Nevertheless, initial research has shown that these carbon nanostructures and their composites with magnetic particles possess unique mechanical and electronic properties, leading to their potential application in different important areas, such as adsorbents,⁸ catalysis support,⁹ hydrogen storage,¹⁰ drug delivery,^{11,12} lithium ion batteries¹³ and microelectronic technologies.¹⁴ Recently, it has been demonstrated that the 2-D carbon nanostructures can be used as field-effect transistors.¹⁵ Therefore, simple methods for the fabrication of these carbon nanostructures on a large scale are promising for their further applications.

Solid-state pyrolysis has been considered an alternative route to produce carbon materials, for its simplicity and high yield.^{16–18} In this process, the metal ions (catalyst) firstly bonded with the carbon precursor followed by heating treatment at certain temperature. Thus, the morphology of the carbon nanostructures may be tuned through changing the type of the carbon source, metal catalysis and their combination mode. The polymers, such as phenolic formaldehyde resin,¹⁹ polystyrene²⁰ and polyurethane²¹ could be used as the carbon precursor for synthesizing the carbon nanostructures *via* the solid-state pyrolysis route. Compared with common polymers, the ion-exchange resin has abundant tunnels with tuned functional organic groups that can adsorb metal ions from various species and with various charge. Consequently, it is possible to control the morphology of the carbon materials obtained by using ion-exchange resins as carbon source. In this communication, we report a simple, economical and large-scale method to prepare various graphitic carbon nanostructures by adopting ion-exchange resins as carbon source. The results

demonstrated that carbon nanocapsules, nanoplates and nanosheets could be easily prepared by simply changing the type of ion-exchange resins and metal salts. To our best knowledge, the controllable synthesis of these carbon materials from a facile and low-cost method still remains a key challenge to date.

The carbon nanostructures were obtained from pyrolysis of different ion-exchange resin–metal ions complexes. The carbon nanocapsules could be obtained by adopting a polyacrylic weak-base anion-exchange (PAWBA) resin as carbon precursor and K₃[Fe(CN)₆] as catalyst source, while changing PAWBA resin to a polystyrenic strong-base anion-exchange (PSSBA) resin, resulted in the formation of plate-like carbon nanostructures. In addition, the carbon nanosheets could be obtained from polyacrylic weak-acid cation-exchange (PAWAC) resin and FeCl₂ salts. (The basic structures of the ion-exchange resins and detailed synthetic processes about various carbon nanostructures are listed in the ESI.[†])

All the samples after treatment with concentrated HCl were examined by transmission electron microscopy (TEM). Fig. 1a shows the TEM images of the sample resulting from PAWBA-[Fe(CN)₆]^{3–} complex after carbonization at 1100 °C under N₂ ambient for 30 min. It can be seen that the sample

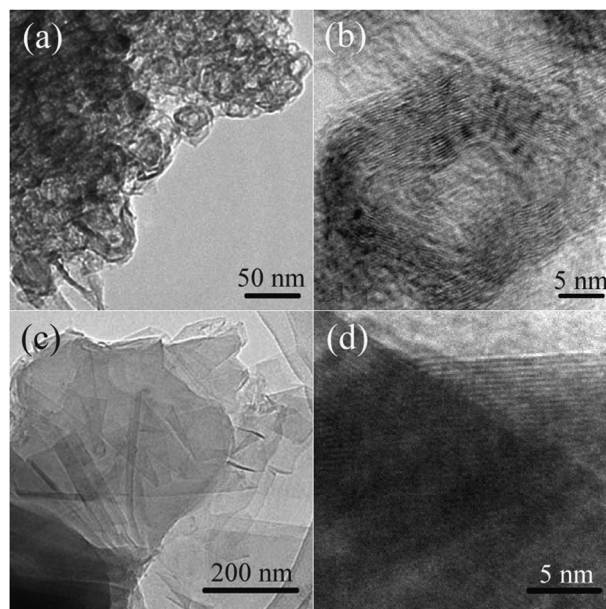


Fig. 1 TEM images of the carbon nanocapsules (a) and nanosheets (c), the HRTEM images of carbon nanocapsules (b) and nanosheets (d).

Laboratory of Physical Chemistry, School of Chemistry and Materials Science, Heilongjiang University, Harbin, 150080, P. R. China.
E-mail: fuhg@vip.sina.com; Fax: +86-451-86608458;

Tel: +86-451-86608458

† Electronic supplementary information (ESI) available: Basic structures of the ion-exchange resins and detailed synthetic processes about various carbon nanostructures. See DOI: 10.1039/b810500f

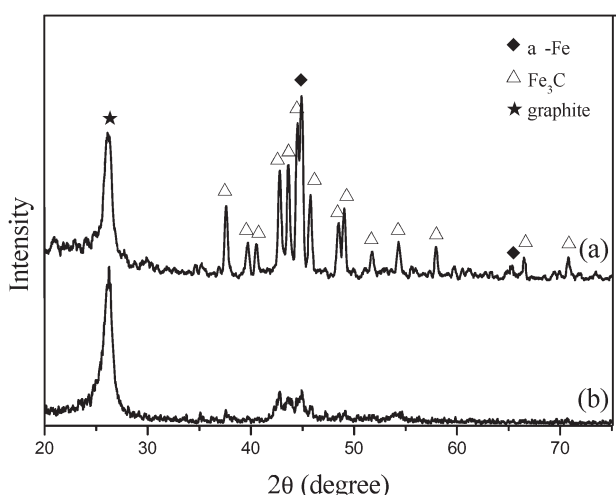


Fig. 2 XRD patterns of the carbon nanocapsules before (a) and after (b) treatment with concentrated HCl.

consists of homogeneous capsules with inner diameters of around 15 nm, and the outer diameters in the range of 30 to 40 nm. High-resolution TEM (HRTEM) images depicted in Fig. 1b show the walls are composed of graphite sheets and the interlayer spacing in the walls is about 0.34 nm, which corresponds to the (002) distance of a graphitic carbon lattice, implying that the carbon in the sample is well crystalline. The components of the sample were characterised using X-ray diffraction (XRD). In Fig. 2a, the diffraction peaks located at $2\theta = 26.2^\circ$ are characteristic of a crystalline graphite (002) plane, further demonstrating the graphitization of carbon in the sample. In addition, magnetic particles Fe_3C and α -Fe also exist in this sample. The results showed formation of magnetic particles/carbon capsule composite by a solid-state pyrolysis process. After treatment with concentrated HCl, the diffraction peaks of Fe_3C and α -Fe are very weak as shown in Fig. 2b. The result demonstrated that most of the magnetic particles were removed and the obtained sample is mainly composed of the graphitic carbon nanocapsules.

Instead of PAWBA with PSSBA, without changing other experimental parameters, plate-like carbon nanostructures but not carbon capsules were obtained. The electron beam transparent features suggest that the carbon nanostructure are very thin as shown in Fig. S2a.[†] From the HRTEM shown in Fig. S2(b),[†] it can be seen that the interlayer spacing is about 0.34 nm which is characteristic of the (002) planes of graphitic carbon. XRD study indicates that the product is mainly composed of graphite, Fe_3C and α -Fe (Fig. S3).[†] The result shows the important effect of resin type on the carbon materials morphology. To obtain the carbon nanostructures with other morphology, the types of resin and metal salt were simultaneously changed. Fig. 1c gives TEM images of the sample prepared by carbonization of PAWAC- Fe^{2+} composites under the same pyrolysis conditions. The stacked areas of two or more nanosheets could be distinctly seen, suggesting successful preparation of very thin carbon nanosheets. The lattice fringe spacing of 0.34 nm calculated from Fig. 1d agrees well with the (002) plane spacing of graphitic carbon. Also, the XRD pattern (Fig. S5)[†]

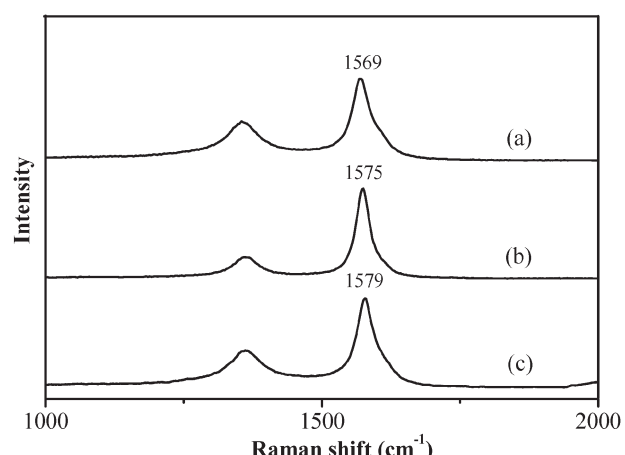


Fig. 3 Raman spectra of the carbon nanocapsules (a), carbon nanosheets (b) and carbon nanoplates (c).

demonstrates that the sample was composed of graphite and α -Fe. The intensive diffraction at $2\theta = 26.2^\circ$ implies that the carbon in the sample is well graphitized. The results showed that the change allowed synthesizing carbon material with novel morphology.

Raman spectroscopy is one of the effective tools for obtaining information about the carbon nanostructures. The peak positions are related not only to crystallines but also to the morphology of carbon nanostructures. Fig. 3a shows the Raman spectrum of the carbon nanocapsules. Two peaks at 1357 and 1569 cm⁻¹ are characteristic of a symmetry breakdown at the edge of graphene sheets (D-band) and the E_{2g} vibrational mode of graphite layers (G-band), respectively. For carbon nanosheets (Fig. 3b) and carbon nanoplates (Fig. 3c), the two peaks are located at 1362, 1579 cm⁻¹ and 1360, 1575 cm⁻¹, respectively. It is well known that the D-band is closely related to the disorder-induced scattering resulting from imperfections or the loss of hexagonal symmetry of the carbon nanostructures, while the G-band is related to the vibration of sp^2 -bonded carbon atoms in a two-dimensional (2D) hexagonal lattice. The intensity ratio between G and D bands (I_G/I_D) is a usual measurement of the graphitic ordering. Two visible features can be observed from the Raman spectra. First, all of the I_G/I_D values are larger than 2.0, suggesting a high degree of graphitization of these carbon structures, which is consistent with the results obtained from HRTEM and XRD. Second, the peaks of G bands for carbon nanoplates and nanosheets have a down-shift (1 and 5 cm⁻¹, respectively) compared to the highly oriented pyrolytic graphite (HOPG, 1580 cm⁻¹). While for the carbon nanocapsules, the shift is up to 11 cm⁻¹. The results are consistent with previous reports about Raman spectra of highly curved graphitic carbon capsules and carbon-plane nanostructures.²²

In the synthesis, the metal ions firstly coordinated to the organic functional group of the ion-exchange resin to form the corresponding resin–metal ions complexes. Afterward, the complexes were pyrolyzed to form certain carbon nanostructures and the metal ions transferred into magnetic particles simultaneously. In order to more thoroughly explore the phase formation and transfer process of metal and carbon, a series of

experiments have been done using carbon nanoplates as a model. Fig. S3† shows XRD patterns of the PAWBA-[Fe(CN)₆]³⁻ samples after carbonization at different temperatures. From the patterns it can be seen that no obvious diffraction peaks of graphite were observed until the temperature reached 600 °C. As the temperatures were increased to 700 °C, the diffraction peak of graphite can be observed. The relative intensity of the peak is enhanced with the increase of reaction temperature. On the other hand, the metal precursor undergoes series of phase/state changes along with that of the carbon precursor. As the reaction temperature reached 500 °C, no crystalline phase of ferric compounds was detected. With increasing the temperature to 600 °C, new phases of Fe₃C and α-Fe are formed. Subsequently, the main phases of the products are composed of graphite, Fe₃C and α-Fe until 1100 °C. The phase formation and transfer processes of the carbon also were reflected by Raman spectra (Fig. S4). The two peaks at 1362 and 1579 cm⁻¹ were observed, and the intensity ratio of I_G/I_D grew gradually with the increase of reaction temperature, indicating increase of the graphic degree of carbon.

The above-mentioned results indicate the formation of different graphitic carbon nanostructures by simply changing the types of carbon source and metal catalyst. An issue could arise concerning the formation of different graphitic carbon structures in the present study. Based on our experimental results, the reason may be ascribed to the different structures of various ion-exchange resins (Fig. S1).† The analysis showed that the Fe content in products containing carbon nanosheets and nanocapsules are about 57.8 and 28.1% (Table S2),† respectively. Also, the steric hindrance of the organic group in the PAWAC-Fe²⁺ complex is less than that of the PAWBA-[Fe(CN)₆]³⁻ complex. Thus, for carbon nanosheets, it is envisaged that the catalyst particles could “consecutively” arrange with small clearance, leading to forming of “consecutive” 2-D carbon nanostructures. The formation of carbon nanocapsules may be attributed to larger steric hindrance of the organic group in the PAWAB-[Fe(CN)₆]³⁻ complex, low Fe content in the product. Also, the carbonyl group in the composites could be decomposed to produce different gases (CO₂ and CO) under heating, which is favorable for the formation of carbon nanostructures with a hollow interior, such as CNTs.²³ Although the Fe contents for carbon nanocapsules and nanoplates are similar, the absence of oxygenous gas during the carbonization of PSSBA-[Fe(CN)₆]³⁻ may be the reason for the formation of plate-like carbon nanostructures possessing a similar size to that of carbon nanocapsules.

In summary, a simple strategy was developed for the controllable preparation of graphitic carbon nanocapsules, nanoplates and nanosheets on a large scale. The simultaneous formation of magnetic particles with carbon nanostructures allowed to obtain magnetic separated carbon materials that have a potential application for adsorption and separation (see Fig. S6).† Although the real processes for the formation of different carbon nanostructures are difficult to clarify, the success was attributed to the variety of structures and the exchange ability of ion-exchange resins. Also, the primary experiments showed that the other novel

carbon nanostructures can be obtained by replacement of Fe salts with Ni or Co salts. Further work on studying the effect of more experimental parameters and understanding the formation mechanism is underway. The method is promising due to its simple operation, large-scale production and easy tune of morphology from readily available and inexpensive starting materials.

The work was supported by the Key Program Projects of the National Natural Science Foundation of China (No 20431030), the National Natural Science Foundation of China (No 20671032), the Key Program Projects of the Province Natural Science Foundation of Heilongjiang Province (No ZJG0602-01) and the Programme for New Century Excellent Talents in University (NCET-04-0341).

Notes and references

- 1 S. Iijima, *Nature*, 1991, **354**, 56.
- 2 P. Poncharal, Z. L. Wang, D. Ugarte and W. A. de Heer, *Science*, 1999, **283**, 1513.
- 3 J. J. Wang, M. Y. Zhu, R. A. Outlaw, X. Zhao, D. M. Manos and B. C. Holloway, *Carbon*, 2004, **42**, 2867.
- 4 Z. H. Kang, E. B. Wang, B. D. Mao, Z. M. Su, L. Gao, S. Y. Lian and L. Xu, *J. Am. Chem. Soc.*, 2005, **127**, 6534.
- 5 G. Mpourmpakis, E. Tylianakis and G. E. Froudakis, *Nano Lett.*, 2007, **7**, 1893.
- 6 X. Lu and Z. Chen, *Chem. Rev.*, 2005, **105**, 3643.
- 7 D. Tasis, N. Tagmatarchis, A. Bianco and M. Prato, *Chem. Rev.*, 2006, **106**, 1105.
- 8 N. H. Phan, S. Rio, C. Faur, L. L. Coq, P. L. Cloirec and T. H. Nguyen, *Carbon*, 2006, **44**, 2569.
- 9 O. C. Carneiro, P. E. Anderson, N. M. Rodriguez and R. T. K. Baker, *J. Phys. Chem. B*, 2004, **108**, 13307.
- 10 A. D. Lueking, R. T. Yang, N. M. Rodriguez and R. T. K. Baker, *Langmuir*, 2004, **20**, 714.
- 11 K. Ajima, M. Yudasaka, T. Murakami, A. Maigné, K. Shiba and S. Iijima, *Mol. Pharm.*, 2005, **2**, 475.
- 12 Z. Guo, L. L. Henry and E. J. Podlaha, *Electrochem. Soc. Trans.*, 2006, **1**, 63.
- 13 W. M. Zhang, J. S. Hu, Y. G. Guo, S. F. Zheng, L. S. Zhong, W. G. Song and L. J. Wan, *Adv. Mater.*, 2008, **20**, 1160.
- 14 J. S. Bunch, A. M. van der Zande, S. S. Verbridge, I. W. Frank, D. M. Tanenbaum, J. M. Parpia, H. G. Craighead and P. L. McEuen, *Science*, 2007, **315**, 490.
- 15 X. R. Wang, Y. J. Ouyang, X. L Li, H. L. Wang, J. Guo and H. J. Dai, *Phys. Rev. Lett.*, 2008, **100**, 206803.
- 16 A. M. Herring, J. T. Mckinnon, B. D. McClosky, J. Filley, K. W. Gneshin, R. A. Pavelka, H. J. Kleebe and D. J. Aldrich, *J. Am. Chem. Soc.*, 2003, **125**, 9916.
- 17 N. A. Katcho, E. Urones-Garrote, D. Avila-Brande, A. Gomez-Herrero, S. Urbonaite, S. Csillag, E. Lomba, F. Agullo-Rueda, A. R. Landa-Canovas and L. C. Otero-Diaz, *Chem. Mater.*, 2007, **19**, 2304.
- 18 M. Zhao, H. H. Song, X. H Chen and W. T. Lian, *Acta Mater.*, 2007, **55**, 6144.
- 19 S. J. Han, Y. Yun, K. W. Park, Y. E. Sung and T. Hyeon, *Adv. Mater.*, 2003, **15**, 1922.
- 20 K. Chen, C. L. Wang, D. Ma, W. X. Huang and X. H. Bao, *Chem. Commun.*, 2008(24), 2765.
- 21 Z. Guo, S. Park, H. T. Hahn, S. Wei, M. Moldovan, A. B. Karki and D. P. Young, *Appl. Phys. Lett.*, 2007, **90**, 053111.
- 22 E. D. Obiuztsova, M. Fujii, S. Hayashi, V. L. Kuznetsov, Y. V. Butenko and A. L. Chuvilin, *Carbon*, 1998, **36**, 821.
- 23 L. Y. Chen, J. F. Bai, C. Z. Wang, Y. Pan, M. Scheer and X. Z. You, *Chem. Commun.*, 2008(13), 1581.